Universal Filtered OFDM with Filter Shift Keying

(*Invited Paper*)

Selahattin Gokceli, Ertugrul Basar, Gunes Karabulut Kurt

Wireless Communications Research Laboratory
Department of Electronics and Communication Engineering
Istanbul Technical University, Istanbul, Turkey
{gokcelis, basarer, gkurt}@itu.edu.tr

***Abstract*—Due to its several implementation advantages, orthogonal frequency division multiplexing (OFDM) has become the most frequently used waveform in modern wireless communication technologies. However, OFDM has some vulnerabilities that may limit its advantages. In order to alleviate OFDM's vulnerabilities, several waveforms have been proposed within the context of 5G research activities. Universal-filtered OFDM (UF-OFDM) is one of the most effective waveforms due to its OFDM-like structure, easier implementation procedure and robustness against synchronization errors. Most of the recent studies on novel waveforms generally target filter optimization or performance improving techniques. In this paper, as a novel approach, UF-OFDM with filter shift keying (OFDM-FSK) is proposed. Here, we consider the filter realizations to carry information through index modulation mechanism. Accordingly, utilized filter of each UF-OFDM subband is selected from a filter set based on the incoming data bits, and an increase in data rate is obtained. At the receiver side, accumulated maximum-likelihood decision metric in each subband is computed. The filter realization, as well as data symbols, that provide the minimum decision metric in each subband are detected. Hence the throughput of the conventional waveform is increased in an efficient and practical manner. The performance of OFDM-FSK system is evaluated through extensive computer simulations. To assess its real-time performance, real-time experiments are also carried out by using software defined radio (SDR) nodes. In the created testbed, a wireless synchronization structure is provided and the considered waveforms are tested in a setup with imperfect synchronization. This experimentation provides realistic insights about the benefits of OFDM-FSK. As it will be demonstrated via both computer simulation and test results, OFDM-FSK provides significant throughput and error performance benefits over UF-OFDM.**

***Keywords*—5G, filter shift keying, index modulation, OFDM, SDR, UF-OFDM, UFMC.**

I. Introduction

Orthogonal frequency division multiplexing (OFDM) has been the most preferred waveform in modern wireless technologies and will also be the foundational waveform of 5G technology. However, OFDM has some drawbacks, such as high out-of-band emissions and high sensitivity to synchronization errors. The use of OFDM in the emerging short-packet transmission scenarios is also challenging. Several new waveforms have recently been proposed to meet the foreseen requirements. As one of the most effective waveforms, universal-filtered OFDM (UF-OFDM) waveform, which is also known as universal filtered multi-carrier (UFMC), is proposed in [1]. UF-OFDM is more robust against real-time impairments than OFDM. UF-OFDM's main difference from the OFDM waveform is the subband-wise filtering operation, which is implemented by utilizing finite impulse response (FIR) filters. Each subband is considered as a resource block (RB) that includes a group of contiguous subcarriers. After the inverse discrete Fourier transform (IDFT) operation, each subband is filtered by a specific FIR filter. Such procedure brings improved robustness against carrier frequency offset (CFO) and improves its suitability to short-packet transmission scenarios. Due to these advantages, UF-OFDM has been regarded as a candidate waveform for 5G and technologies beyond.

Recent studies on new waveforms mostly focus on error performance improvements by targeting filter optimization or integration of supportive techniques. However, such solutions do not bring any throughput improvement, as the throughput improvement requirements of 5G scenarios currently have not met yet. In this study, to address this fundamental problem, a novel UF-OFDM with filter shift keying (OFDM-FSK) scheme is proposed. In OFDM with index modulation (OFDM-IM) technique, which is proposed in [2] and practically implemented in [3], in addition to the ordinary data symbols, additional data bits are also transmitted with the selection of active subcarrier indices. This transmission technique provides various improvements over OFDM. Inspired by this approach, in this study, a subband-wise filtering operation is considered as a data transmission mechanism. A methodology that provides throughput improvement without causing any loss in conventional benefits of UF-OFDM, is proposed. The success of OFDM-FSK system depends on the selection of proper filter sets that contain distinguishable FIR filters. A detector that can easily be implemented, is utilized on the receiver side, and the corresponding data symbols and the FIR filter that provide the minimum accumulated decision metric in subband, are detected. Bit error performance of the system is evaluated by both computer simulations and real-time experiments, which are carried out by software defined radio (SDR) nodes and a wireless synchronization procedure is implemented to perform more realistic experiments. This procedure allows us to analyze the OFDM-FSK system's performance in the presence of real-time impairments, including synchronization errors.

The rest of the paper is organized as follows. In Section II, the relevant studies in the literature are summarized. In Section III, system model of the proposed technique is given. The details of created testbed, computer simulations and test results are presented in Section IV. Finally, the paper is concluded in Section V.

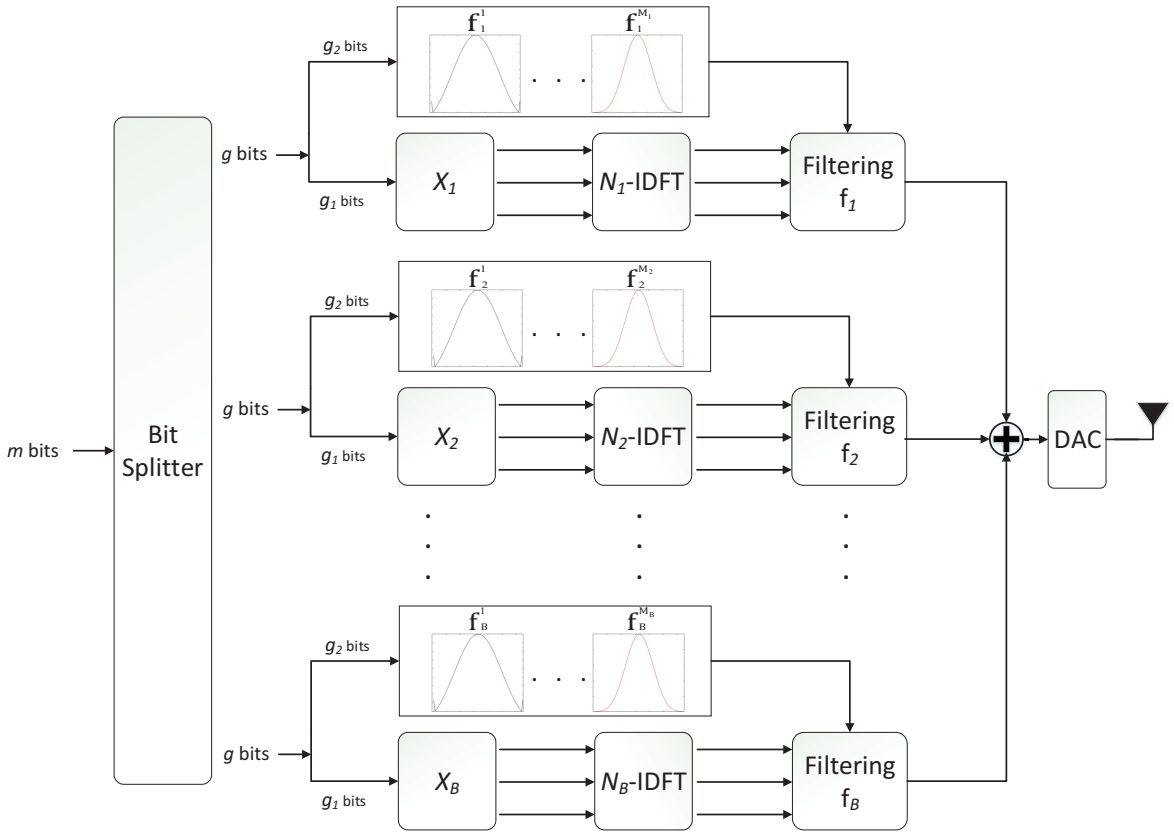

Fig. 1: Block diagram of the transmitter.

II. Related Works

In addition to UF-OFDM, as an alternative to OFDM, several waveforms have been proposed within the context of 5G research activities. One effective waveform is filter bank multicarrier (FBMC), which includes subcarrier-wise filtering. Such filtering provides considerably low sidelobes and renders FBMC more robust against synchronization errors than OFDM [4]. However, long signal tails caused by subcarrier-wise filtering, and its implementation complexity limit the usage of FBMC in real-time. As another candidate, generalized frequency division multiplexing (GFDM) is proposed in [5]. GFDM has subcarrier-wise filtering and non-orthogonal subcarrier localization, and provides low out-of-band emissions. This benefit renders GFDM suitable to cognitive radio applications. In [6], filtered OFDM (f-OFDM) is proposed. Similar to the principle of UF-OFDM, subband-wise filtering is also utilized in f-OFDM, where the filter length is allowed to exceed the cyclic prefix (CP) length. However, the relatively long symbol duration limits the applicability of f-OFDM to some 5G scenarios that require short-packet transmissions. The authors of [7] present a comparison of OFDM, GFDM and UF-OFDM in cognitive radio applications. Accordingly, UF-OFDM and GFDM waveforms provide a better performance than that of OFDM. Similarly, OFDM, GFDM, FBMC and UF-OFDM waveforms are experimented in [8] under timing offset (TO) and CFO. It is demonstrated that UF-OFDM and linear FBMC provide the best performance among these waveforms. These studies demonstrate that UF-OFDM is a rational and an effective choice for 5G and beyond applications.

The literature on UF-OFDM waveform studies mostly include the optimization of FIR filters to obtain various benefits. In [9], suppression of out-of-subband emission is targeted to improve the disadvantages of conventional FIR filters. Similarly, [10] focuses on limiting out-of-subband emission and filter optimization. Moreover, in [11], in order to improve the robustness of UF-OFDM against synchronization errors, filter optimization is utilized and filter emissions are constrained. Beyond these, there are other interesting approaches. For example, RB size and filter length are optimized to obtain improved signal reception in [12]. However, to the best of the authors' knowledge, there is no study that contains the novel filter-based data transmission methodology, which is proposed in this study.

III. System Model

In this section, we present the transceiver structure of the proposed OFDM-FSK scheme. Block diagram of the transmitter implementation is shown in Fig. 1. First, the incoming m information bits are divided into B groups of g bits, i.e., $B = m/g$. In conventional UF-OFDM, incoming bits of each group are modulated using M-QAM symbols and the corresponding subband is created from these symbols. However, FSK methodology enables the transmission of additional data bits and g is higher for the FSK system compared to the conventional UF-OFDM model. In the FSK system, g bits consist of g_1 conventional data bits that are modulated to M-QAM symbols, and g_2 filter modulation (shift keying) bits

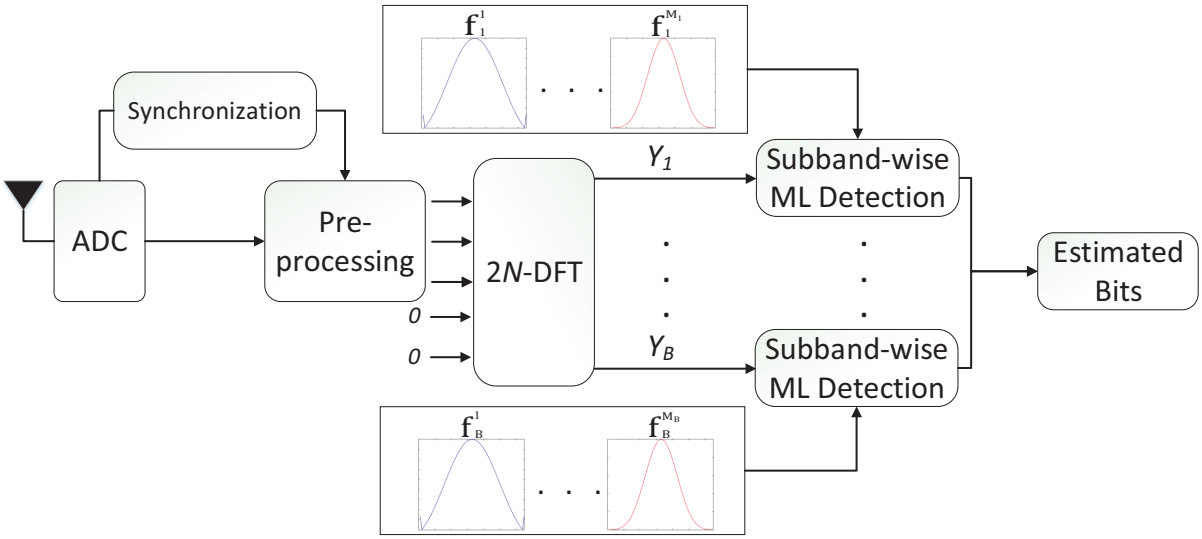

Fig. 2: Block diagram of the receiver.

that determine the realized FIR filter $\mathbf{f}_i^s$ that contains time-domain low-pass prototype filter coefficients, from the filter set $\mathcal{F}_i = \{\mathbf{f}_i^1, \mathbf{f}_i^2, \ldots, \mathbf{f}_i^{M_i}\}$, where $i \in \{1, 2, \ldots, B\}$ represents the index of the subband and M_i represents the total number of available filters at the implementation of i^{th} subband. Filters in the set $\mathcal{F}_i$, can be selected as Dolph-Chebyshev filters with the same length L; however, with different sidelobe attenuation levels. In this study, the same filter set is utilized in all subbands and the total number of available filters is represented as M_f, i.e., $M_1 = M_2 = \cdots = M_B = M_f$. Moreover, OFDM-FSK system is represented by considering the filter setup as OFDM-M_f-FSK.

Let g_1 bits constitute N_i frequency domain M-QAM symbols $X_i[k]$, $k \in \{0, 1, \ldots, N-1\}$, with the total N_i subcarriers. The time-domain symbol at the i^{th} subband is obtained after N-point IDFT as

$$\tilde{x}_i[n] = \frac{1}{\sqrt{N}} \sum_{n=0}^{N-1} X_i[k]\, e^{j2\pi kn/N}, \quad n = 0, 1, \ldots, N-1. \tag{1}$$

Then, the filtering operation is implemented by using the selected filter $\mathbf{f}_i^s$ such that

$$\mathbf{x}_i = \tilde{\mathbf{x}}_i * \mathbf{f}_i^s, \tag{2}$$

where $\tilde{\mathbf{x}}_i = [\, \tilde{x}_i[0]\ \tilde{x}_i[1]\ \cdots\ \tilde{x}_i[N-1]]$, $*$ is the linear convolution operator, and the length of the selected filter $\mathbf{f}_i^s$ is represented by L. Afterwards, each filtered signal in subbands are summed and the UF-OFDM symbol is obtained as

$$\mathbf{x} = \sum_{i=1}^{B} \tilde{\mathbf{x}}_i. \tag{3}$$

The block diagram of the receiver implementation is presented in Fig. 2. First, the transmitted signal is received from wireless channel as

$$y[n] = h[n] * x[n] + w[n], \quad n = 0, 1, \ldots, N+L-1, \tag{4}$$

where $x[n]$ represents the n^{th} component of $\mathbf{x}$, $h[n]$ represents the channel impulse response and $w[n]$ represents the additive white Gaussian noise (AWGN) component. Then, zero-padding is performed and the length of the time-domain signal is increased to $2N$ in order to implement $2N$-point DFT. With this operation, $Y[k]$, the frequency domain representation of $y[n]$, is obtained. Then, subband-wise detection procedure is implemented. To properly detect the transmitted ordinary bits and filter modulation bits, subband-wise detection procedure is used, where subcarriers at the corresponding indices of the subband are grouped and $Y_i[k]$ is created. After this step, by considering all possible filter realizations $\mathbf{f}_i^s$, maximum-likelihood (ML) detection is implemented on each subband. Each minimum decision metric value, which is obtained from ML detection on the corresponding subcarrier, is kept and summed to determine the filter that provides the minimum decision metric in a given subband. Finally, transmitted ordinary data subcarriers and utilized filter are detected. This procedure can be represented as

$$\{\hat{X}_i[k], \hat{\mathbf{F}}_i^s\} = \arg \min_{\mathbf{F}_i^s \in \mathfrak{F}_i, S[a] \in \mathcal{M}_i} \sum_{k=I_i[0]}^{I_i[N_{B_i}]} \left| \frac{Y_i[k]}{F_i^s[k]} - H_i[k] S[a] \right|^2, \tag{5}$$

where $\mathfrak{F}_i$ is the frequency domain representation of the filter set $\mathcal{F}_i$, $\mathbf{I}_i$ is the index vector that contains N_{B_i} subcarrier indices of the corresponding subband, $\mathcal{M}_i$ represents the utilized M_i-QAM constellation at the i^{th} subband and $S[a]$ represent the a^{th} symbol of this constellation. Moreover, $\mathbf{F}_i^s$ consists of $F_i^s[k]$, i.e., $\mathbf{F}_i^s = [\, F_i^s[0]\ F_i^s[1]\ \cdots\ F_i^s[N-1]]$. Note that in this study, all subbands contain symbols from the same constellation. Moreover, $Y_i[k]$ and $H_i[k]$ represent the received frequency domain signal and the corresponding channel coefficient, respectively. The success of the detection procedure depends on the distinguishability of individual filters in the filter set $\mathcal{F}_i$. This detector exploits the filter parameter differences between the possible filters and at the end, chooses the optimal one.

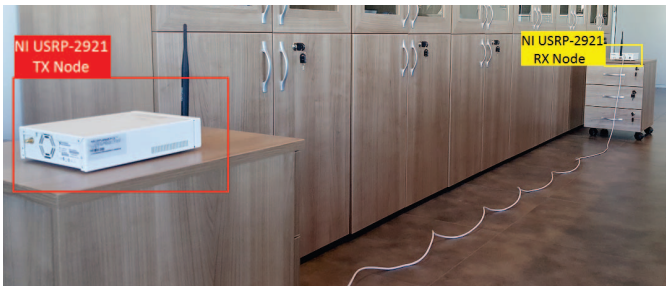

Fig. 3: Experimental setup used in real-time implementation.

TABLE I: Measurement setup parameters.

Carrier frequency	2.45 GHz
I/Q data rate	10^6 samples/sec
Sampling rate ($1/T_s$)	1.25×10^6 samples/sec
Utilized modulation	4-QAM
Number of data subcarriers	160
Number of reference subcarriers	20
Zero padding / DFT length (N)	76 / 256
Filter length (L)	65
Number of subbands (B)	20 / 40
Subband size (N_B)	4 / 8
Sidelobe levels of filters (dB)	$\{30, 40, 50, 60, 70, 80, 90, 100\}$
Simulation Channel	4-tap Rician, $K = 5$ uniform power delay profile
Distance between Tx and Rx nodes	4 meters

IV. Simulation and Test Results

In this section, details of the created testbed, as well as computer simulation and test results are presented. In Fig. 3, the realized experimental setup is shown. This testbed includes two NI USRP-2921 nodes. Since a multicarrier transmission is realized, synchronization of the system is crucial. This is achieved by a configured wireless synchronization procedure. Accordingly, each node has GPSDO module that provides a 10 MHz reference and 1 PPS signal, and an iterative CFO estimation procedure is utilized to synchronize these modules wirelessly. Programming of transmitter and receiver implementations is performed by using LabVIEW and its virtual instrument (VI) components. Details of this procedure are skipped for brevity. Interested readers are referred to [13] in which a similar procedure can also be found. Channel estimation is implemented by a transmission of block symbols and zero-forcing detector. For CFO and TO estimation, a technique, which is proposed for UF-OFDM in [13], is used. Similarly, signal-to-noise ratio (SNR) estimation is also achieved by following the same methodology in the referenced study.

Parameters that are used in computer simulations and real-time experiments are shown in Table I. Performances of considered waveforms are measured in terms of bit error rate (BER). As the first experimentation case, data transmission is realized by FSK in the absence of ordinary data transmission through M-QAM. In this way, performance benefits of pure FSK are investigated. Computer simulation and real-time experiment results for this case are shown in Fig. 4. Note that due to functional limitations of the devices, a limited range is experimented in real-time for energy per bit to noise power spectral density ratio (E_b/N_0). Two subband size configurations are considered to observe the trade-off between BER and throughput. Moreover, three different configurations are

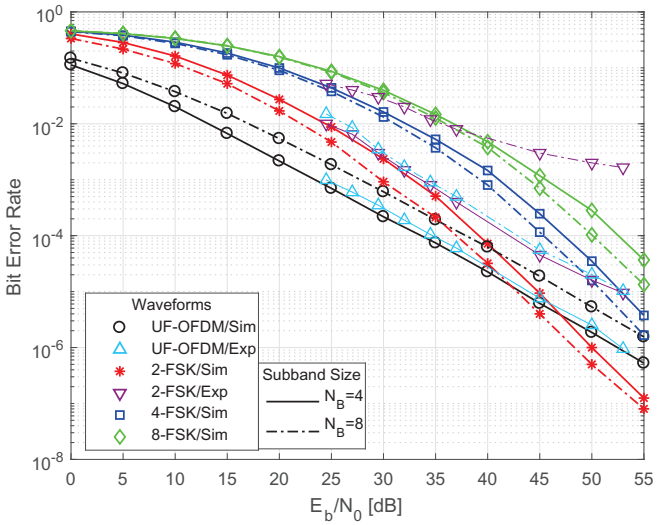

Fig. 4: Performance results of the case of FSK modulation without ordinary data transmission.

experimented for $\mathcal{F}_i$. These are two, four and eight available filters, respectively. As observed, the higher throughput, which is obtained with $N_B = 4$, results in degraded BER when compared to the case of $N_B = 8$ for all three filter size configurations. The performance differences between these increase when the FSK size increases from two to eight. When conventional UF-OFDM waveforms are compared, $N_B = 4$ provides a better error performance. Therefore, it is clear that FSK operation changes this difference. An important observation is that when two filters are included in $\mathcal{F}_i$, the performance of FSK systems outperforms that of UF-OFDM waveforms, especially after E_b/N_0 of 35 dB. This shows FSK's effectiveness at high E_b/N_0 values, which may be critical for ultra-reliable applications. In Fig. 4, real-time performance results are also presented. Accordingly, performance of FSK system starts to degrade due to existence of CFO and channel estimation errors, and UF-OFDM provides better results. However, 2-FSK with $N_B = 4$ has a better error performance than that of UF-OFDM with $N_B = 8$. Therefore, it can be concluded that if channel estimation error becomes dominant, a careful design in the FSK system may provide a more robust error performance. Moreover, the case of $N_B = 4$ provides a better error performance that the case of $N_B = 8$, which can be explained with channel characteristics of the experimented testbed and suitability of pilot pattern in the case of $N_B = 4$ to these characteristics.

As the second step, BER performances of OFDM-FSK and UF-OFDM waveforms are evaluated by both computer simulations and real-time experiments. Results for the cases of $N_B = 4$ and $N_B = 8$ are shown in Figs. 5 and 6, respectively. Again, three different FSK configurations are experimented. Bandwidth of the transmission is equal to 1 MHz and, subcarrier spacing is approximately 5.56 kHz, which results in a symbol duration of 0.18 ms. Therefore, in captions of Figs. 5 and 6, bit rate (R) is $\frac{Bg}{T_s} = \frac{320}{0.18\times10^{-3}} = 1.78$ Mbits/sec. Throughput improvements that are obtained with different number of available filters are also shown in these figures. When N_B is equal to 4, BER degrades slightly

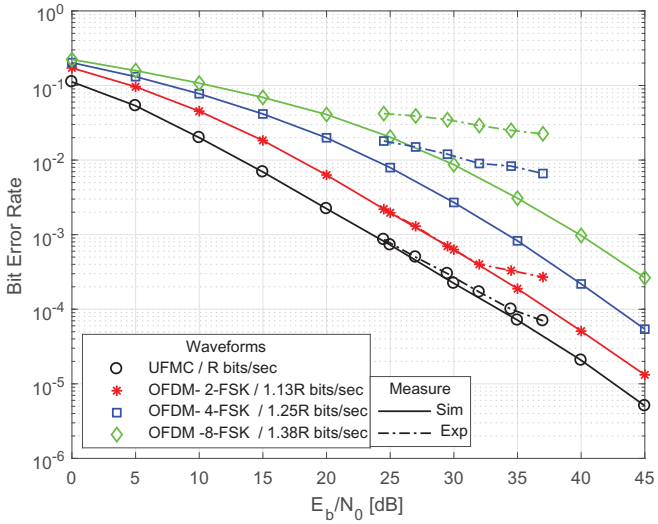

Fig. 5: Performance results of the OFDM-FSK and UF-OFDM waveforms for $N_B = 4$.

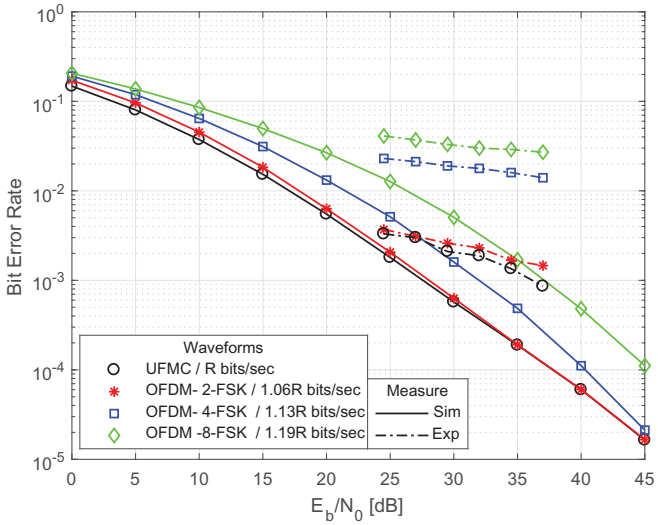

Fig. 6: Performance results of the OFDM-FSK and UF-OFDM waveforms for $N_B = 8$.

with the increase of the number of experimented filters from two to eight. Especially for two filters, an acceptable BER performance with a good throughput improvement is obtained. When N_B is equal to 8, satisfactory BER performances as well as throughput improvements over UF-OFDM waveform are obtained. Specifically for two filters, almost the same performance is obtained with a throughput increase. In case of four filters, a satisfactory amount of throughput increase is obtained. As observed from real-time performance results, the differences in performance are in accordance with results that are obtained with computer simulations. It is clear that OFDM-2-FSK is more robust to real-time impairments compared to the other FSK setups. When compared with UF-OFDM, OFDM-2-FSK waveform performs similarly without significant error performance loss, at the same time, this scheme provides a significant throughput improvement.

V. Conclusion

In this study, a novel OFDM-FSK waveform has been proposed by exploiting the filtering operation itself as a data transmission source to increase the throughput. An efficient and practical transmission structure has been proposed. Several parameters have been experimented to assess the potential benefits of the OFDM-FSK waveform. As observed with comprehensive computer simulations and real-time experiments, OFDM-FSK waveform provides a notable throughput improvement without sacrificing error performance. These results are promising for the potential real-time applicability of OFDM-FSK, and significant gains can be obtained with this waveform in 5G technologies and beyond. As the future work, more distinguishable filters and more advanced transmission structures will be investigated.

Acknowledgement

The work of E. Basar was supported by the Turkish Academy of Sciences Outstanding Young Scientist Award Programme (TUBA-GEBIP).

References

[1] T. Wild, F. Schaich, and Y. Chen, "5G air interface design based on universal filtered (UF-)OFDM," in *Proc. 2014 19th Int. Conf. on Digital Signal Process.*, Aug. 2014, pp. 699–704.

[2] E. Basar, U. Aygolu, E. Panayirci, and H. V. Poor, "Orthogonal frequency division multiplexing with index modulation," *IEEE Trans. Signal Process.*, vol. 61, no. 22, pp. 5536–5549, Nov. 2013.

[3] S. Gokceli, E. Basar, M. Wen, and G. K. Kurt, "Practical implementation of index modulation-based waveforms," *IEEE Access*, vol. 5, no. 1, pp. 25 463–25 473, Dec. 2017.

[4] B. Farhang-Boroujeny, "OFDM versus filter bank multicarrier," *IEEE Signal Process. Mag.*, vol. 28, no. 3, pp. 92–112, May 2011.

[5] G. Fettweis, M. Krondorf, and S. Bittner, "GFDM - Generalized frequency division multiplexing," in *Proc. IEEE 69th Veh. Tech. Conf.*, Apr. 2009, pp. 1–4.

[6] J. Abdoli, M. Jia, and J. Ma, "Filtered OFDM: A new waveform for future wireless systems," in *Proc. IEEE 16th Int. Workshop on Signal Process. Advances in Wireless Commun. (SPAWC)*, June 2015, pp. 66–70.

[7] M. Danneberg, R. Datta, A. Festag, and G. Fettweis, "Experimental testbed for 5G cognitive radio access in 4G LTE cellular systems," in *Proc. 2014 IEEE 8th Sensor Array and Multichannel Signal Process. Workshop (SAM)*, June 2014, pp. 321–324.

[8] A. Aminjavaheri, A. Farhang, A. RezazadehReyhani, and B. Farhang-Boroujeny, "Impact of timing and frequency offsets on multicarrier waveform candidates for 5G," in *Proc. 2015 IEEE Signal Process. and Signal Process. Education Workshop (SP/SPE)*, Aug. 2015, pp. 178–183.

[9] M.-F. Tang and B. Su, "Filter optimization of low out-of-subband emission for universal-filtered multicarrier systems," in *Proc. 2016 IEEE Int. Conf. on Commun. Workshops (ICC)*, May 2016, pp. 468–473.

[10] X. Wang, T. Wild, F. Schaich, and A. F. dos Santos, "Universal filtered multi-carrier with leakage-based filter optimization," in *Proc. 20th European Wireless Conf.*, May 2014, pp. 1–5.

[11] X. Wang, T. Wild, and F. Schaich, "Filter optimization for carrier-frequency- and timing-offset in universal filtered multi-carrier systems," in *IEEE Xth Veh. Tech. Conf. (VTC Spring)*, May 2015, pp. 1–6.

[12] H. Kim, J. Bang, S. Choi, and D. Hong, "Resource block management for uplink UFMC systems," in *Proc. 2016 IEEE Wireless Commun. and Netw. Conf.*, Apr. 2016, pp. 1–4.

[13] S. Gökceli, B. Canli, and G. K. Kurt, "Universal filtered multicarrier systems: Testbed deployment of a 5G waveform candidate," in *Proc. 2016 IEEE 37th Sarnoff Symp.*, Sep. 2016, pp. 94–99.